

SUPPLEMENTARY FIGURES

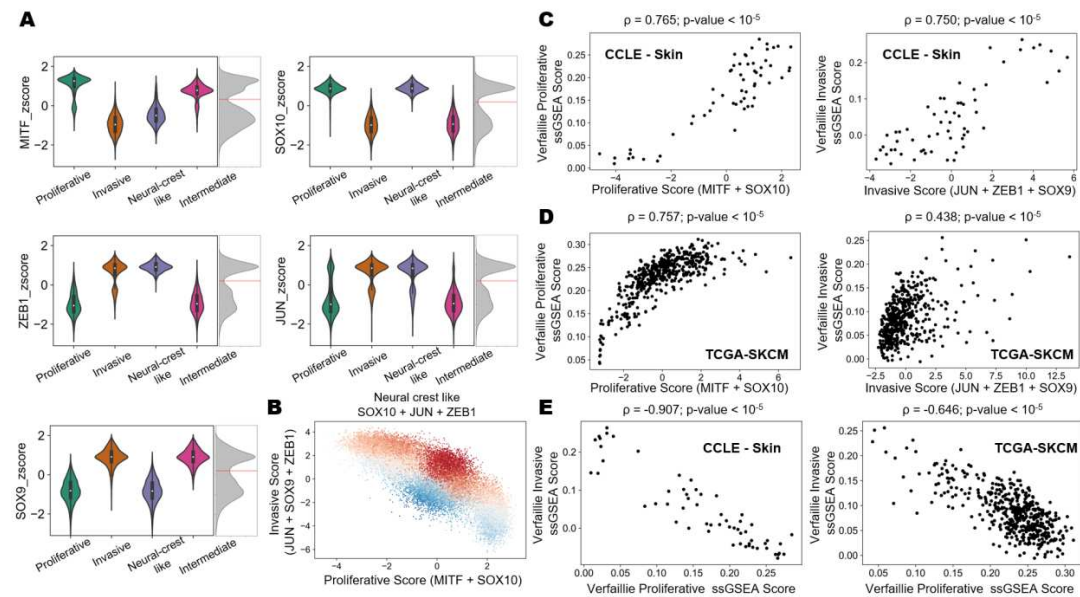


Figure S1: Characteristic gene expression profiles of master regulators for different phenotypes and benchmarking against Verfaillie scores. **A)** Violin plots of z-normalized steady state gene expression values of MTF, SOX10, ZEB1, JUN and SOX9 grouped by cluster labels obtained from hierarchical clustering. Kernel density estimates for steady state expression of master regulators showing bimodality, partitioned by red line. **B)** Scatter plot showing the spread of steady state solutions with Proliferative score on x-axis and Invasive score on y-axis. The steady states have been colored by Neural crest like scores. **C)** Scatter plot comparing five gene based proliferative and invasive score against ssGSEA score for Verfaillie proliferative (left) and invasive gene signatures (right) in CCLE group of skin cancer cell lines. **D)** Scatter plot comparing five gene based proliferative and invasive score against ssGSEA score for Verfaillie proliferative (left) and invasive gene signatures (right) in TCGA cohort of SKCM patients. **E)** Scatter plot showing association between Verfaillie proliferative and invasive ssGSEA scores for CCLE group of skin cancer cell lines (left) and TCGA cohort of SKCM patients (right).

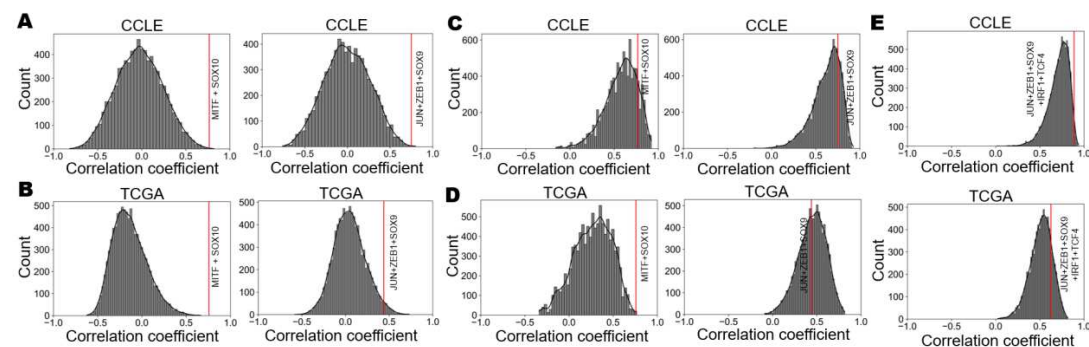


Figure S2: Assessing random gene combination correlations with Verfaillie signatures. **A)** Frequency distribution of correlation coefficients for random combinations of any 2 (left) or 3 (right) transcription factors with Verfaillie proliferative (left) and invasive (right) gene signature ssGSEA scores in the CCLE skin cancer cell line group. **B)** Same as A) but for TCGA SKCM patient cohort. **C)** Frequency distribution of correlation coefficients for random combinations of 2 (left) or 3 (right) transcription factors chosen from within the Verfaillie proliferative (left) and invasive (right) signatures in the CCLE skin cancer cell line group. **D)** Same as C) but for TCGA SKCM patient cohort. Red line indicates the correlation of proliferative score (MITF+SOX10) with the Verfaillie proliferative

signature (left) and the correlation of invasive score (SOX9+ZEB1+JUN) with the Verfaillie invasive score in A, B, C, and D. E) Frequency distribution of correlation coefficients for random combinations of 5 transcription factors chosen from within the Verfaillie invasive signature in CCLE skin cancer cell line group (top) and TCGA SKCM patient cohort (bottom). The red line represents the correlation of the refined invasive score (SOX9+ZEB1+JUN+IRF1+TCF4) with the Verfaillie invasive score.

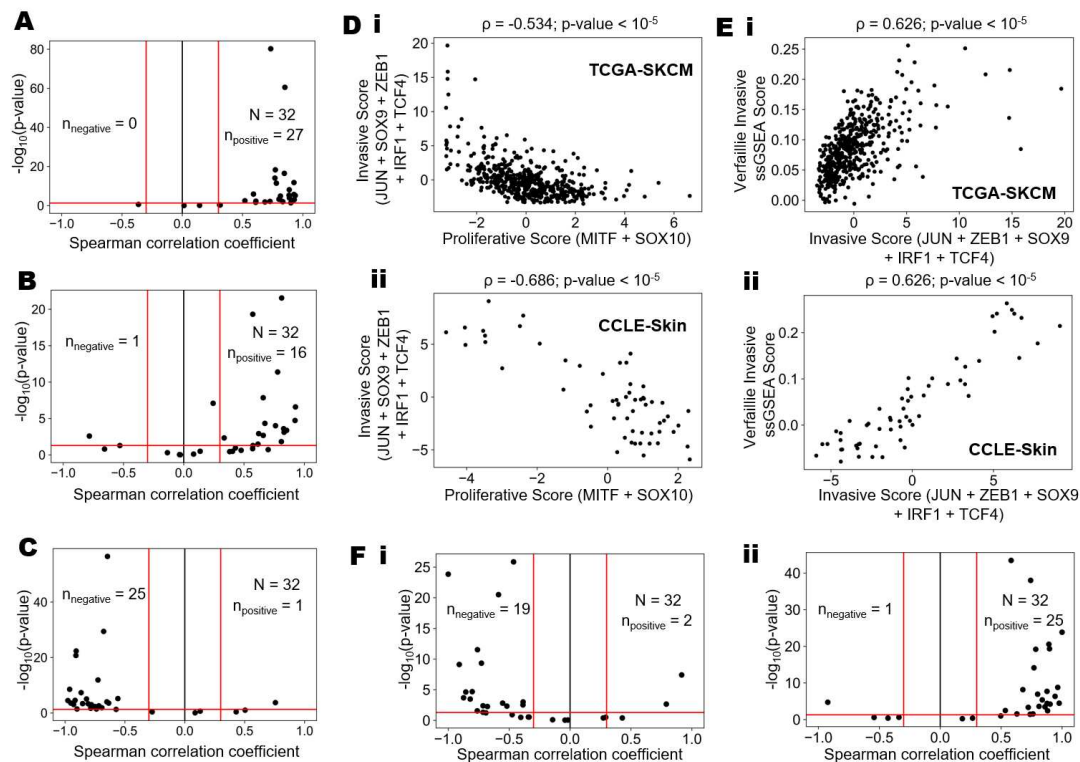


Figure S3: Meta-analysis of melanoma datasets. A) Volcano plots showing correlation of two-gene based proliferative score with Verfaillie proliferative gene signature based ssGSEA score B) Volcano plots showing correlation of three-gene based invasive score with Verfaillie invasive gene signature based ssGSEA score C) Volcano plots showing correlation of Verfaillie proliferative ssGSEA score with Verfaillie invasive ssGSEA score, for all bulk transcriptomics datasets. $n_{negative}$ and $n_{positive}$ denote the number of datasets (out of 32) that are correlated negatively (Spearman correlation coefficient < -0.3 ; p -value < 0.05) and positively (Spearman correlation coefficient > 0.3 ; p -value < 0.05). D) Scatterplot showing association between the proliferative (MITF+SOX10) and invasive (SOX9+ZEB1+JUN+IRF1+TCF4) scores for clinical samples from i) TCGA cohort of SKCM patients ii) CCLE-skin cell lines. E) Scatter plot comparing five gene based invasive score against ssGSEA based Verfaillie invasive score in i) TCGA cohort of SKCM patients ii) CCLE-skin cell lines. F) Volcano plot for the results of meta-analysis of melanoma datasets, accounting for the associations between the i) proliferative (MITF+SOX10) and invasive scores (SOX9+ZEB1+JUN+IRF1+TCF4) ii) invasive scores (SOX9+ZEB1+JUN+IRF1+TCF4) with Verfaillie invasive gene signature based ssGSEA score; $n_{negative}$ and $n_{positive}$ denote the number of datasets (out of 32) that are correlated negatively (Spearman correlation coefficient < -0.3 ; p -value < 0.05) and positively (Spearman correlation coefficient > 0.3 ; p -value < 0.05)

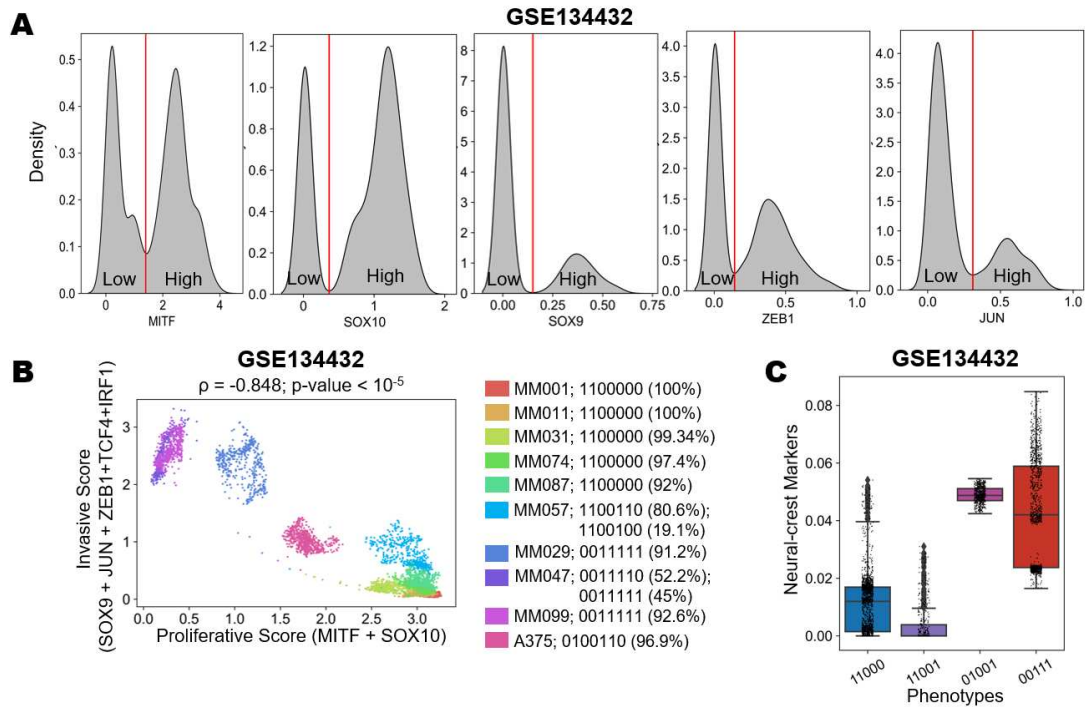


Figure S4: Single-cell transcriptomics data analyses. **A)** Density distributions for expression of master regulators- MITF, SOX10, SOX9, ZEB1, JUN as see in the single cell RNA-seq dataset GSE134432. The red line partitions the expression profiles of these genes to high and low levels at the major minima of each distribution. **B)** Scatterplot of single cell RNAseq data showing each cell of each cell line projected on a proliferative-invasive plane define by proliferative (MITF+SOX10) and invasive (SOX9+ZEB1+JUN+IRF1+TCF4) imputed scores. **C)** Boxplots of cells categorized by the dominant binary phenotypes based on the five gene signature and ssGSEA scores based on Neural-crest markers (GSE134432).

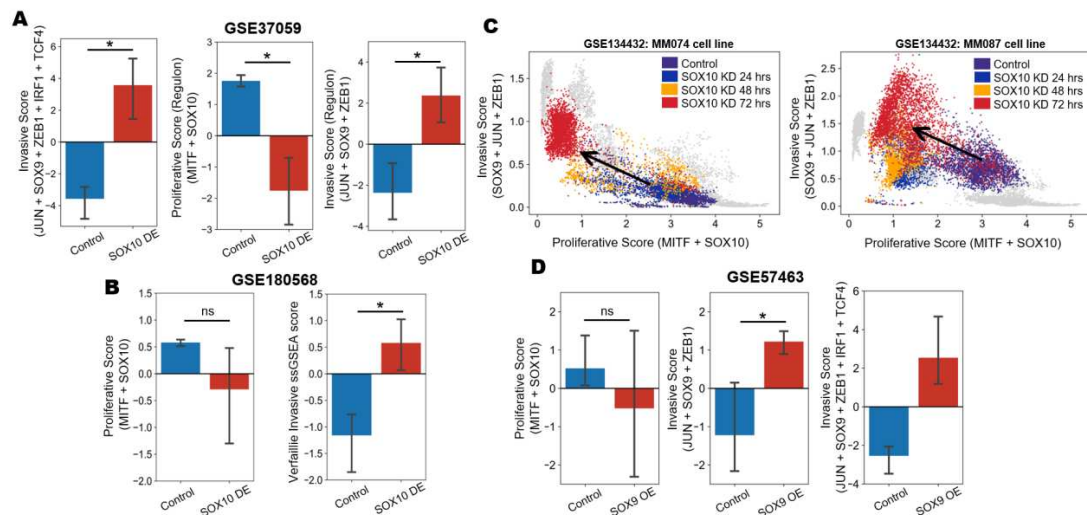


Figure S5: Transcriptomics data in support of transitions along the proliferative-invasive axis upon experimental perturbations. **A)** Bar plots of the experimentally observed significant changes (demarcated by *) in the five gene based invasive scores with TCF4 and IRF1 (left), in the proliferative (defined as the sum of z-normalized ssGSEA scores of MITF and SOX10 regulons) (middle) and invasive scores (defined as the sum of z-normalized ssGSEA scores of JUN, ZEB1 and SOX9 regulons) (right) upon SOX10 down expression in comparison to control case (GSE37059). **B)** Bar plots showing changes in proliferative (left) and invasive (right) scores upon SOX10 down expression (GSE180568). **C)** Scatter plots showing the spread of cells of MM074 (left) and MM087 (right) cell line as they transition along the proliferative-invasive 2D plane over a period of 72 hours of SOX10 siRNA treatment. **D)** Bar plots showing experimentally observed changes in the proliferative score (left) and three-gene based invasive score (middle) and refined five-gene based (right) upon SOX9 over expression (GSE57463).

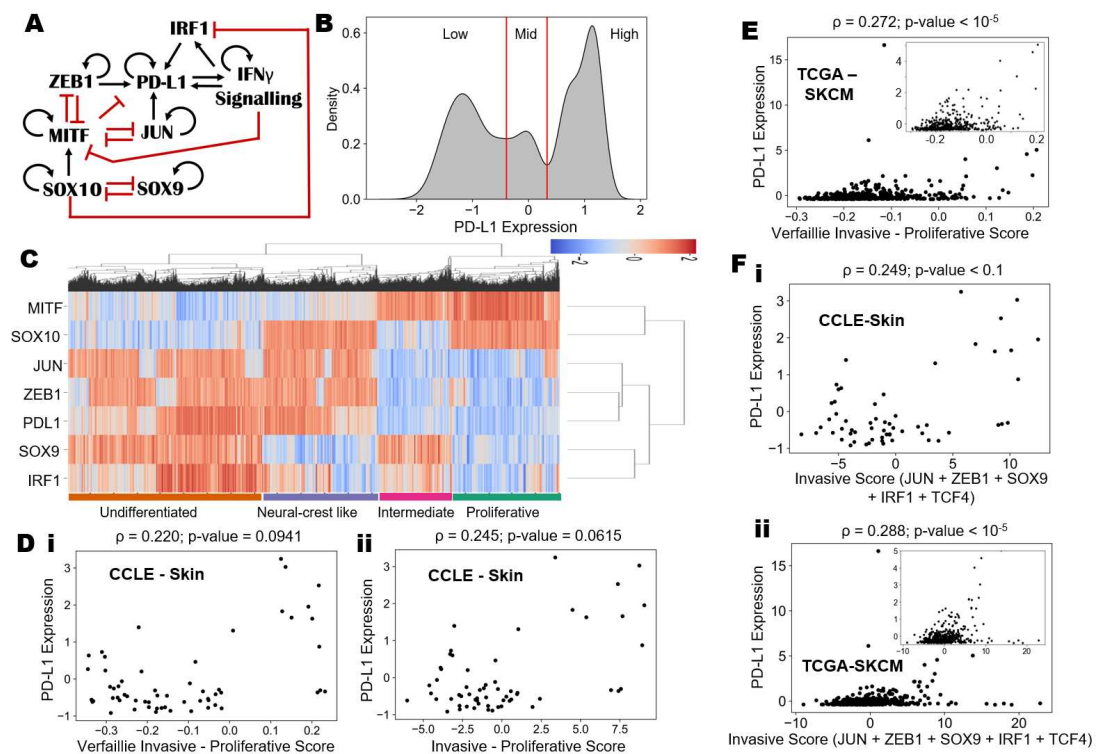


Figure S6: Refining the regulatory network with IRF1 and relation of PD-L1 expression with refined invasive score. **A)** Enhanced gene regulatory network incorporating IRF1 into the previous circuit. **B)** Density histogram of PD-L1 expression fitted with kernel density estimate showing a trimodal distribution. Red lines show the partition between PD-L1 expression levels being high, mid, and low. **C)** Hierarchically clustered heatmap of simulated steady states permitted by the new gene regulatory network and qualitative classification of the four emerging cell states. The simulated four phenotypes have been labelled. **D)** Scatterplot showing associations between the i) Verfaillie Invasive – Proliferative scores and ii) 5 gene signature based invasive – proliferative scores with PD-L1 levels. **E)** Scatterplot showing associations between the Verfaillie Invasive – Proliferative scores with PD-L1 levels in the TCGA cohort of melanoma patients. **F)** Scatterplot showing the association of invasive score with TCF4 and IRF1 and PD-L1 expression for i) CCLE group of skin cancer cell lines ii) TCGA cohort of SKCM patients.

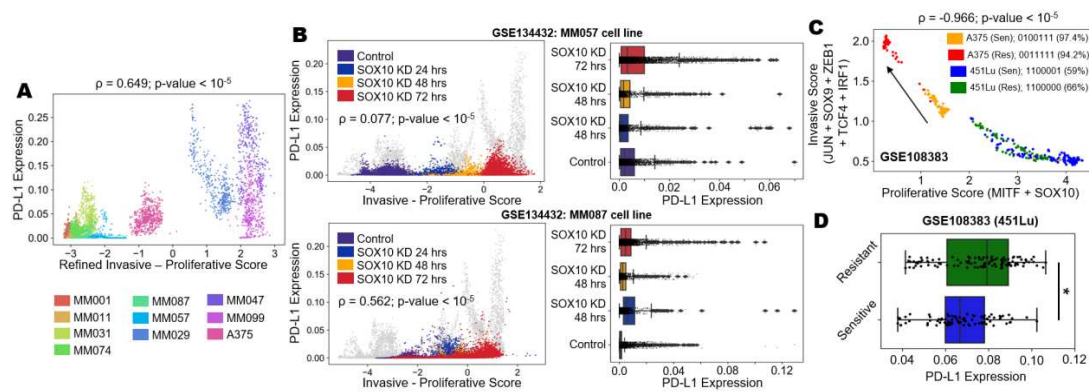


Figure S7: Associations between PD-L1 levels and proliferative-invasive nature of melanoma cells.

A) Scatterplot showing the association of PD-L1 expression with the new (added IRF1 and TCF4) invasive-proliferative score axis in GSE134432. **B)** Scatter plot and corresponding boxplots showing changes in PD-L1 levels of SOX10 knockdown cells in MM057 (top) and MM087 (bottom) cell lines as they transition from a proliferative phenotype to an invasive phenotype along 24h, 48h and 72h time course single cell RNA-seq data in comparison to control data (GSE134432). **C)** Scatterplot of single cell RNA-seq data projecting cells of two cell lines – A375 (red and orange corresponding to the resistant and sensitive clones, respectively) and 451Lu (green and blue corresponding to the resistant and sensitive clones, respectively) on the refined proliferative-invasive plane. **D)** Box plot showing differences in PD-L1 levels in the sensitive and resistant clones of 451Lu melanoma cells. * represents a statistically significant difference in the levels based on Student's *t*-test.

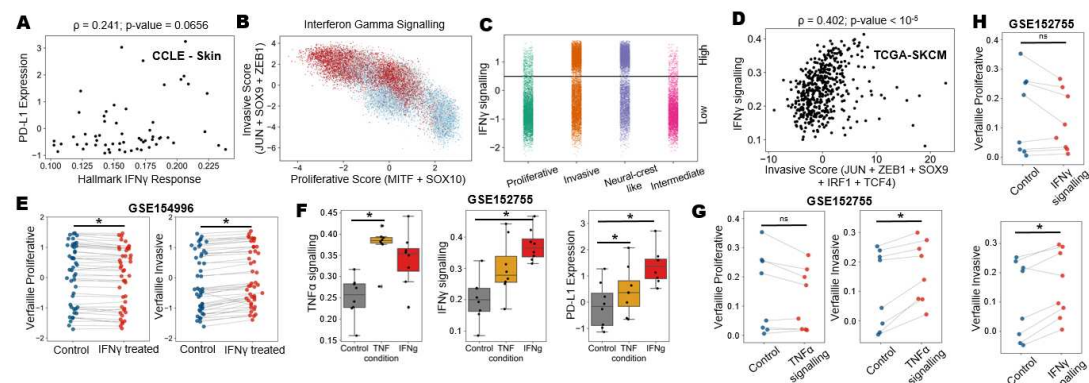


Figure S8: Characterizing association of IFN γ signaling with PD-L1 levels and proliferative invasive nature of melanoma cells. **A)** Scatter plots showing association between Hallmark IFN γ response on x-axis and PD-L1 expression on y-axis for CCLE group of skin cell lines. **B)** Scatter plot showing all the steady states projected onto the proliferative - invasive plane colored based on IFN γ signaling levels. **C)** Strip plot showing the PD-L1 steady state levels for the 4 phenotypes. The horizontal lines mark the stratification of IFN γ signaling levels into low and high regions. **D)** Scatterplot showing the association between IFN γ signaling and invasive score including TCF4 and IRF1 in TCGA cohort of SKCM patients. **E)** Paired plot showing the changes in levels of i) Verfaillie proliferative and ii) Verfaillie Invasive activity levels when wild type melanoma cells are treated with IFN γ . **F)** Boxplot showing levels of Hallmark TNF α , Hallmark IFN γ signalling and PD-L1 levels in 8 melanoma cells treated with either TNF or IFN γ . Paired plot showing the changes in levels of Verfaillie proliferative and Verfaillie Invasive activity levels when wild type melanoma cells are treated with **G)** TNF or **H)** IFN γ . * represents a statistically significant difference in the levels based on a paired Student's *t*-test while ns represents a non-significant difference.

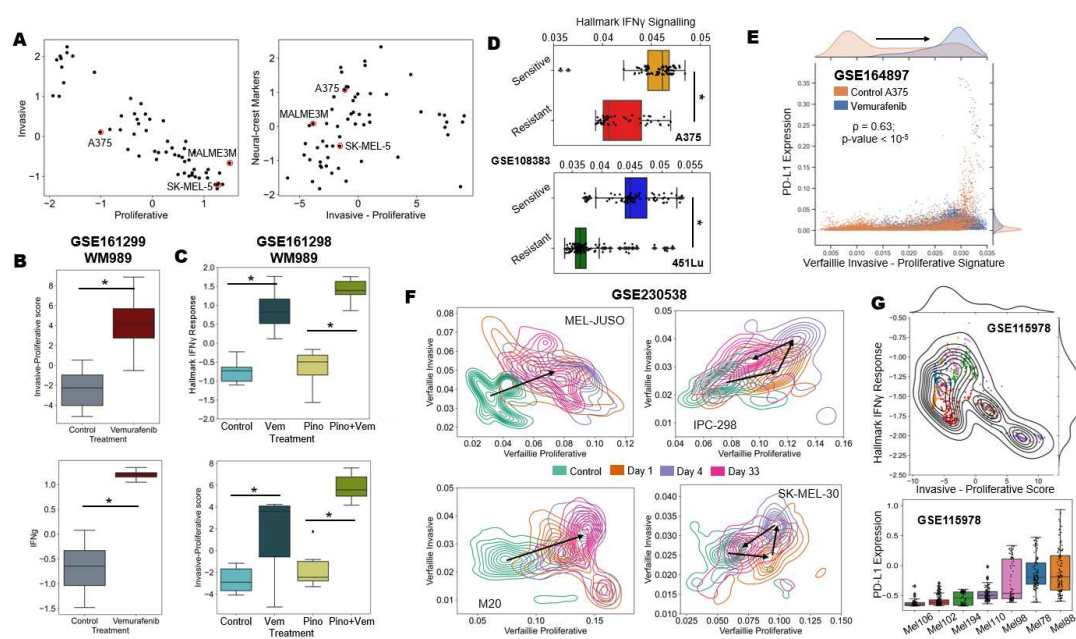


Figure S9: Impact of targeted therapy and immunotherapy on interplay among PD-L1 levels, proliferative to invasive transition and IFN γ signaling. A) Scatterplots showing the association between Verfaillie proliferative and invasive score (left) and proliferative to invasive transition score with Neural crest ssGSEA score (right) in CCLE skin cancer cell line. Cell lines selected for experimentation (SK-MEL-5, MALME-3M, A375) on basis of their proliferative-invasive status are highlighted in red circles. B) Box plots showing changes along the proliferative-invasive axis (top) and IFN γ signaling (bottom) upon vemurafenib treatment (GSE161299). C) Box plots showing changes along the proliferative-invasive axis (top) and IFN γ signaling (bottom) upon vemurafenib treatment alone and in combination with pinometostat (GSE161298). D) Box plots showing changes in Hallmark IFN γ signaling in sensitive and resistant clones of A375 (top) and 451Lu (bottom) melanoma cells. E) Scatterplot showing modest PD-L1 levels upon vemurafenib treatment (GSE164897). F) Contour maps showing transitions on the proliferative-invasive plane after treatment with MEK inhibitors and CDK4/6 inhibitors for 4 different cell lines (GSE230538). G) Scatterplot of single cells from melanoma patients after treatment with immune checkpoint inhibitor therapy projected on the Invasive-Proliferative score and Hallmark IFN γ signaling and their corresponding PD-L1 levels in a patient specific grouping sorted ascending order according to median expression values. Each color in the scatterplot corresponds to a particular patient sample.